

Beyond the Waterbed Effect: Development of Fractional Order CRONE Control with Non-Linear Reset

Linda Chen, Niranjan Saikumar, Simone Baldi and S. Hassan HosseinNia

Abstract—In this paper a novel reset control synthesis method is proposed: CRONE reset control, combining a robust fractional CRONE controller with non-linear reset control to overcome waterbed effect. In CRONE control, robustness is achieved by creation of constant phase behaviour around bandwidth with the use of fractional operators, also allowing more freedom in shaping the open-loop frequency response. However, being a linear controller it suffers from the inevitable trade-off between robustness and performance as a result of the waterbed effect. Here reset control is introduced in the CRONE design to overcome the fundamental limitations. In the new controller design, reset phase advantage is approximated using describing function analysis and used to achieve better open-loop shape. Sufficient quadratic stability conditions are shown for the designed CRONE reset controllers and the control design is validated on a Lorentz-actuated nanometre precision stage. It is shown that for similar phase margin, better performance in terms of reference-tracking and noise attenuation can be achieved.

I. INTRODUCTION

In high-tech industry not only (sub)nanometre precision positioning control, but also high bandwidth is essential: this is the case for wafer scanners used for production of integrated circuits, atomic force microscopes for scanning of dynamic biological samples and printing of three-dimensional nano-structures. It is in demanding cases such as these that requirements for robustness begin to conflict with requirements for reference-tracking, disturbance rejection and noise attenuation, as a result of a fundamental trade-off between robustness and performance. This trade-off is well-studied in the waterbed effect [1] and considered in precision positioning system design [2],[3].

Loop shaping is the industry-standard for control design which allows for performance evaluation in frequency domain. High open-loop gain at low frequency is required for better tracking and effective rejection of disturbances (like external vibrations) and low gain is required at high frequency for precision with better noise attenuation. On the other hand, better robustness of the system is achieved for more phase around bandwidth. Bode's gain-phase relation imposes a direct constraint between the gain and phase behaviour. Thus if the phase is increased in the frequency range around bandwidth as to increase robustness, low-frequency open-loop gain has to decrease and high-frequency

open-loop gain has to increase accordingly, degrading performance of the system. PID controllers, which have been an industry-standard for many years, do not satisfy the ever increasing demands on robustness and performance. By using a fractional order controller such as CRONE [4], additional tunability allows for improved controller design. However, fundamental limitations of linear control remain. This motivates the use of non-linear controllers as a way to break the aforementioned trade-offs.

A promising non-linear control technique in this sense is reset control. J.C. Clegg introduced the reset integrator in 1958 and showed using describing function analysis [5] that a 52° phase lead is achieved when compared to a linear integrator for the same -20dB/decade slope. The improvement in performance of linear systems using reset control has been shown in for instance [6] and [7] amongst others. Today, numerous works on reset control theory exist, with practical applications ranging from: hard-drive disk control [8], [9], servomotor control [10], positioning stages [11], [12] and process control [13], [14], [15]. Reset control design and stability of reset systems remain actively researched topics today. A few results include the PI+CI compensator (PI controller with a Clegg integrator) for which a control design framework has been developed in [16] and time-regularized reset controllers for which asymptotic stability has been guaranteed in [17]. In a recent work, sufficient stability conditions based on measured frequency responses are given [18], which aims to elevate the need for solving linear matrix inequalities (LMI) and thus making reset controllers more accessible to control engineers in industry.

Despite the advances mentioned above, a full and accessible framework for reset control synthesis is to the best of the authors' knowledge, still an open problem. In order to improve tunability in reset control, generalization of reset control to fractional order has already been addressed in [19] and [20]. The aim of this research is to incorporate fractional reset theory developed in mentioned works into CRONE design methodology. The novel CRONE reset controller, could simplify reset control design by enabling the use of common loop shaping methods. Motivation of this research direction arises from the possibility to break the fundamental robustness performance trade-off on the one hand and simplifying robust reset control design on the other.

The rest of the paper is organized as follows: background information about CRONE control and reset control is given in section II. In section III the proposed CRONE reset controller is discussed, followed by a stability analysis of the CRONE reset controller provided in section IV. Validation

Linda Chen and Simone Baldi are with the Delft Center for Systems and Control, Delft University of Technology, Delft, The Netherlands lindachen93@gmail.com, S.Baldi@tudelft.nl

Niranjan Saikumar and S. Hassan HosseinNia are with the Department of Precision and Microsystems Engineering, Delft University of Technology, Delft, The Netherlands N.Saikumar@tudelft.nl, S.H.HosseinNiaKani@tudelft.nl

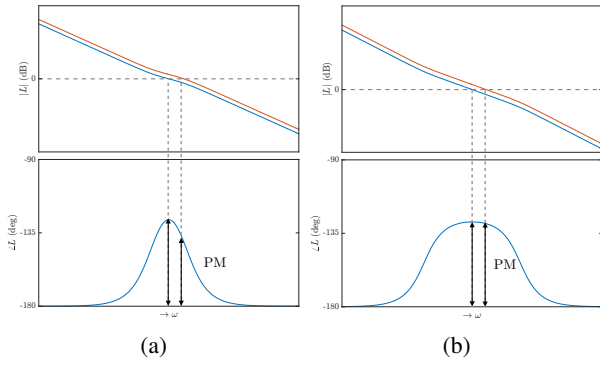


Fig. 1. (a) Typical open-loop response. Under gain variations the phase margin (PM) fluctuates. (b) After achieving constant phase in the frequency range around bandwidth the phase margin is constant.

of the CRONE reset controller on an experimental setup is given in section V followed by a discussion of results in section VI and conclusions in section VII.

II. BACKGROUND

A. CRONE control

In CRONE control robustness against gain deviations in the system is obtained by creating constant phase behaviour around bandwidth in open-loop. This can be seen in Fig. 1. Three generations of CRONE exist today as formalized by [4]. Our focus is on first generation CRONE control (CRONE-1), which can be used for plants with asymptotic phase around bandwidth.

A first generation CRONE controller has a similar transfer function to an integer order series PID controller:

$$C_F(s) = C_0 \left(1 + \frac{\omega_I}{s}\right)^{n_I} \left(\frac{1 + \frac{s}{\omega_b}}{1 + \frac{s}{\omega_h}}\right)^\nu \frac{1}{\left(1 + \frac{s}{\omega_F}\right)^{n_F}} \quad (1)$$

with ω_I and ω_F being the integrator- and low pass filter corner frequencies, ω_b and ω_h the corner frequencies of the band-limited derivative action, $\nu \in \mathbb{R} \cap [0, 1]$ the fractional order and $n_I, n_F \in \mathbb{N}$ being the order of the integrator and low pass filter order respectively. The difference between a series integer order PID controller and a first generation CRONE controller is that the order ν is fractional instead of integer, making first generation CRONE a fractional PID controller. The fractional part of the transfer function can be approximated using Oustaloup approximation within the frequency range. The flat phase behaviour illustrated in Fig. 1b is created by choosing a wider frequency range in which the derivative action is active (compared to PID control) and by decreasing the order ν to a fractional value. This ensures that the gain at high and low frequencies are not affected by the constant phase achieved.

The fractional order ν can be calculated from:

$$\nu = \frac{-\pi + M_\Phi - \arg G(j\omega_{cg}) + n_F \arctan \frac{\omega_{cg}}{\omega_F}}{\arctan \frac{\omega_{cg}}{\omega_b} - \arctan \frac{\omega_{cg}}{\omega_h}} + \frac{n_I \left(\frac{\pi}{2} - \arctan \frac{\omega_{cg}}{\omega_I}\right)}{\arctan \frac{\omega_{cg}}{\omega_b} - \arctan \frac{\omega_{cg}}{\omega_h}} \quad (2)$$

where M_Φ is the required nominal phase margin, ω_{cg} the bandwidth, $G(j\omega)$ is the plant frequency response.

The gain C_0 is chosen such that the loop gain at frequency ω_{cg} is equal to 1.

B. Reset control

A general reset controller can be described by the following impulsive differential equations, using the formalism in [16]:

$$\Sigma_r := \begin{cases} \dot{x}_r(t) = A_r x_r(t) + B_r e(t) & \text{if } e(t) \neq 0, \\ x_r(t^+) = A_\rho x_r(t) & \text{if } e(t) = 0, \\ u(t) = C_r x_r(t) + D_r e(t) & \end{cases} \quad (3)$$

where matrices A_r, B_r, C_r, D_r are the base linear state-space matrices of the reset controller, $e(t)$ is the error between output and reference, $u(t)$ is the control input signal, $x_r(t)$ is the state and A_ρ is the reset matrix. A typical control structure using reset control can be seen in Fig. 2. The overall controller Σ_R consists of a reset controller Σ_r and a linear controller Σ_{nr} . Typical reset elements include the Clegg integrator and the first order reset element (FORE) as in [21]. In the design of a CRONE reset controller, key is to quantify the phase advantage that reset provides: to this purpose, the describing function computation of reset control systems is explained following the formalism of [22].

Describing function: The general describing function of a reset system as defined in [22] is given by:

$$G_{DF}(j\omega) = C_r(j\omega I - A_r)^{-1} B_r (I + j\Theta_D(\omega)) + D_r \quad (4)$$

with $\Theta_D(\omega)$:

$$\Theta_D(\omega) = -\frac{2\omega^2}{\pi} \Delta(\omega) [\Gamma_D(\omega) - \Lambda^{-1}(\omega)] \quad (5)$$

in which the following set of equations are present:

$$\begin{cases} \Lambda(\omega) = \omega^2 I + A_r^2 \\ \Delta(\omega) = I + e^{\frac{\pi}{\omega} A_r} \\ \Gamma_D(\omega) = I + A_r e^{\frac{\pi}{\omega} A_r} \end{cases}$$

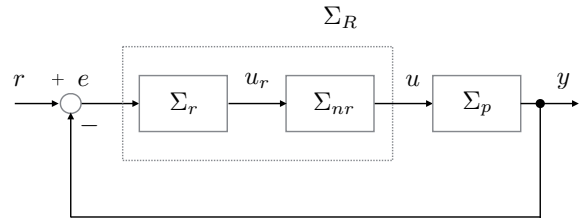


Fig. 2. Control diagram of feedback control with a controller Σ_R , which contains a linear system Σ_{nr} and a non-linear reset system Σ_r .

Creating phase advantage with reset: Using describing function analysis phase and gain behaviour of reset filters can be approximated. Gain behaviour of reset filters very closely resembles that of its linear base filter, whereas phase behaviour can differ significantly. In Fig. 3a, the describing function of the Clegg integrator is compared to the frequency

response of a linear integrator. In Fig. 3b the describing function of a FORE compensator is compared to the frequency response of a first order filter with the same corner frequency of 100Hz. For the reset integrator phase lead is created for all frequencies, whereas for the FORE reduced phase lag is seen after the corner frequency.

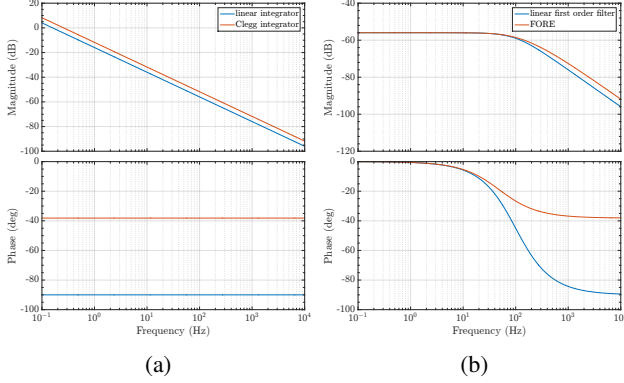


Fig. 3. Describing function of a (a) Clegg integrator and (b) FORE compensator showing less phase lag compared to their linear base transfer functions.

III. CRONE RESET CONTROL

At the base of CRONE reset control is the robust CRONE controller with flat phase behaviour around the bandwidth frequency. With reset action additional phase can be created around bandwidth. When combining CRONE with reset, these two situations would allow for decrease of the open-loop slope around bandwidth by retuning fractional order ν . This has beneficial effects on system performance, as the low-frequency loop gain increases and the high-frequency loop gain decreases as a result. The parameters chosen in the control structure determine the amount of additional phase created by reset. This phase lead is calculated using the describing function and used in the computation of the new fractional order ν . In the subsections below firstly the control structure is explained and then an adapted formula for the fractional order is given.

A. Control structure

The proposed CRONE reset control design structure firstly includes the choice of which part of the CRONE transfer function will be reset. In addition a generalized structure is proposed that allows for tuning the amount of non-linearity versus linearity of the system. The transfer functions below are given for first generation CRONE.

1) CRONE reset strategies:

a) *CRONE integrator reset*: The CRONE integrator reset strategy can be represented by following equation:

$$C_{\text{int}}(s) = \underbrace{\left(\frac{\omega_I}{s}\right)^{n_I-1} C_0 \left(\frac{s}{\omega_I} + 1\right)^{n_I} \left(\frac{1 + \frac{s}{\omega_b}}{1 + \frac{s}{\omega_h}}\right)^\nu}_{\Sigma_{nr}} \frac{1}{\left(1 + \frac{s}{\omega_F}\right)^{n_F}} \times \underbrace{\frac{\omega_I}{s}}_{\Sigma_r} \quad (6)$$

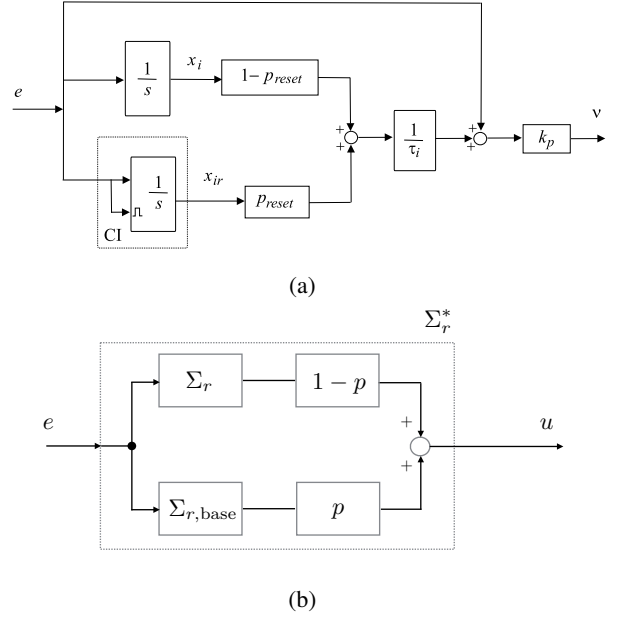


Fig. 4. Block diagram of the (a) PI+CI controller, adapted from [16] and (b) convex combination of the reset controller Σ_r and its linear base controller $\Sigma_{r,\text{base}}$.

in which the integrator part becomes the part that is reset Σ_r and the rest of the transfer function is linear Σ_{nr} .

b) *CRONE first order filter reset*: Similarly, CRONE first order filter reset strategy can be described as:

$$C_{\text{fof}}(s) = \underbrace{\left(\frac{1 + \frac{s}{\omega_h}}{1 + \frac{s}{\omega_b}}\right)^\nu C_0 \left(1 + \frac{\omega_I}{s}\right)^{n_I}}_{\Sigma_{nr}} \frac{1}{\left(1 + \frac{s}{\omega_F}\right)^{n_F}} \frac{1}{1 + \frac{s}{\omega_b}} \quad (7)$$

c) *CRONE lag reset*: Finally, the CRONE lag reset strategy can be described as:

$$C_{\text{lag}}(s) = \underbrace{\left(\frac{1 + \frac{s}{\omega_b}}{1 + \frac{s}{\omega_h}}\right)^{\nu+1} C_0 \left(1 + \frac{\omega_I}{s}\right)^{n_I}}_{\Sigma_{nr}} \frac{1}{\left(1 + \frac{s}{\omega_F}\right)^{n_F}} \frac{1 + \frac{s}{\omega_h}}{1 + \frac{s}{\omega_b}} \quad (8)$$

2) *Two degree of freedom non-linearity tuning controller*: As the CRONE reset controller is designed using describing function, higher harmonics introduced by non-linearity are neglected. However these harmonics do affect the performance of the system. Hence, tuning parameters are needed to control the level of non-linearity introduced in the system. Two different tuning parameters are considered in this work, which will be explained below. Then both methods are used in the proposed control structure.

a) *Reset fraction γ* : In the first method the reset matrix A_p can be taken as $A_p = \gamma I$ [16]. Then the state can be reset to a fraction γ . With $\gamma = 1$, Σ_r becomes linear, whereas with $\gamma = 0$ a full reset occurs. The describing function of a reset integrator is shown in Fig. 6a, and it becomes evident that the reset phase lead can be tuned with γ .

b) *Reset percentage p_{reset}* : The second way of tuning non-linearity in a reset system is using a PI+CI approach

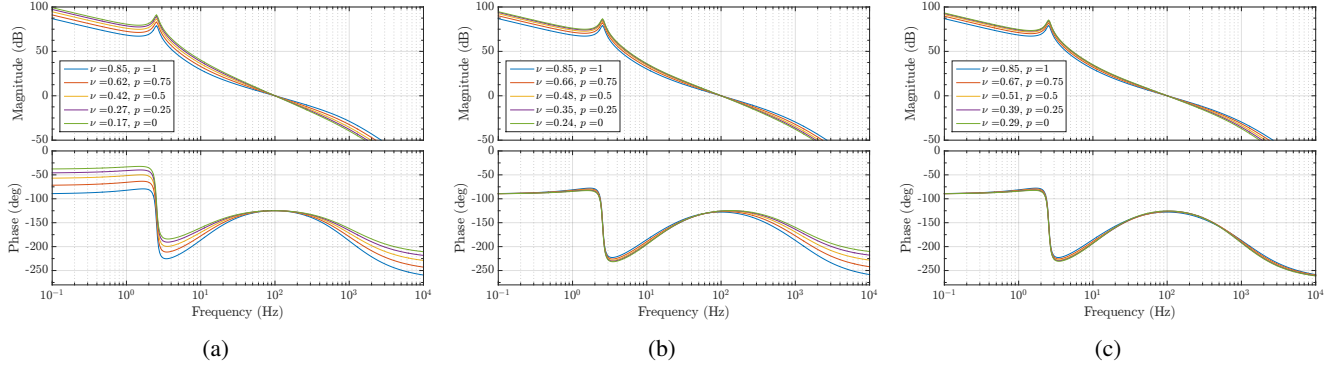


Fig. 5. Open-loop for first generation CRONE with second order plant as in (22) without delay for $\gamma = 0$ and different p -values with (a) integrator reset, (b) first order filter reset and (c) lag reset. For the same phase margin at similar bandwidth the open-loop gain behaviour with reset is favourable.

in the same work of [16], including a reset percentage p_{reset} . This results in a convex combination of a linear integrator and a Clegg integrator. A block diagram of a PI+CI controller can be found in Fig. 4a. The describing function of a reset integrator with varying p_{reset} is shown in Fig. 6b. Intuitively, the amount of phase lead achieved with reset is less when less non-linearity is allowed in the system.

The parallel interconnected system of Σ_r and $\Sigma_{r,\text{base}}$ in Fig. 4b has a more general approach compared to PI+CI : other filters than integrator can be chosen to be combined. Following impulsive differential equations represent this system structure for $\xi = [x_r^T, x_{r,\text{base}}^T]^T$:

$$\Sigma_r^* : \begin{cases} \dot{\xi} = \underbrace{\begin{bmatrix} A_r & 0 \\ 0 & A_r \end{bmatrix}}_{\bar{A}} \xi + \underbrace{\begin{bmatrix} B_r \\ B_r \end{bmatrix}}_{\bar{B}} e, & \text{if } e \neq 0, \\ \xi(t^+) = \underbrace{\begin{bmatrix} \gamma I & 0 \\ 0 & I \end{bmatrix}}_{\bar{A}_\rho} \xi, & \text{if } e = 0, \quad (9) \\ u_r = \underbrace{\begin{bmatrix} (1-p)C_r & pC_r \end{bmatrix}}_{\bar{C}} \xi + \underbrace{D_r}_{\bar{D}} e. \end{cases}$$

Σ_r^* , depicted in Fig. 4b is used instead of Σ_r in the control diagram of Fig. 2. When taking $A_r = \bar{A}$, $B_r = \bar{B}$, $C_r = \bar{C}$, $D_r = \bar{D}$, $A_\rho = \bar{A}_\rho$ and taking (4), the describing function of this controller part can be found. Note that p is taken as $1 - p_{\text{reset}}$ such that with $p = 1$ or $\gamma = 1$ the system is a fully linear system, and full reset if $p = 0$ and $\gamma = 0$.

B. Renewed calculation of fractional order ν

The additional phase at bandwidth is given by $\Phi_r(\omega_{cg})$, which is calculated from:

$$\Phi_r(\omega) = \angle G_{\text{DF}}(j\omega) - \angle G(j\omega) \quad (10)$$

in which $G_{\text{DF}}(j\omega)$ is the describing function of the reset filter and $G(j\omega)$ is the transfer function of its linear base system. Then the new fractional order for first generation CRONE reset ν^* can be calculated as:

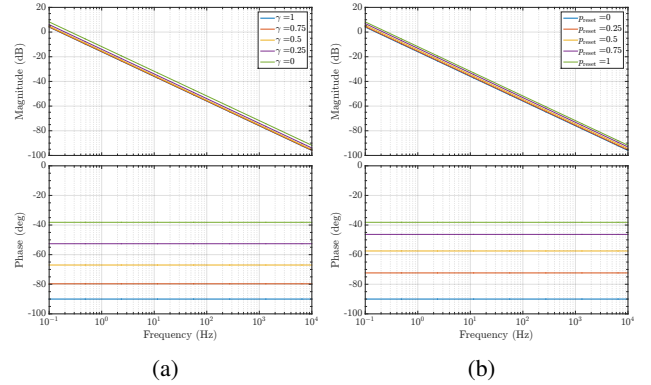


Fig. 6. Describing function of a reset integrator when tuning non-linearity using variable (a) γ and using variable (b) p_{reset} .

$$\nu^* = \frac{-\pi + M_\Phi - \arg G(j\omega_{cg}) + n_F \arctan \frac{\omega_{cg}}{\omega_F}}{\arctan \frac{\omega_{cg}}{\omega_b} - \arctan \frac{\omega_{cg}}{\omega_h}} + \frac{n_I \left(\frac{\pi}{2} - \arctan \frac{\omega_{cg}}{\omega_I} \right) - \Phi_r}{\arctan \frac{\omega_{cg}}{\omega_b} - \arctan \frac{\omega_{cg}}{\omega_h}}. \quad (11)$$

The amount of phase advantage calculated for different reset strategies in first generation CRONE are as follows:

a) CRONE integrator reset

$$\Phi_{r,\text{int}}(p, \gamma) = \arctan \left(\frac{4}{\pi} (1-p) \frac{1-\gamma}{1+\gamma} \right) \quad (12)$$

which is a constant phase for all frequencies when fixing p and γ .

b) CRONE first order filter reset

$$\Phi_{r,\text{fof}}(\omega, p, \gamma, \omega_b) = \arctan \left((1-p) \Theta_D(\gamma, \omega, \omega_b) \right) \quad (13)$$

with $\Theta_D(\gamma, \omega)$ defined as (5).

c) CRONE lag reset

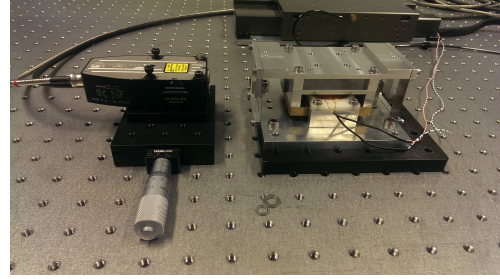
V. EXPERIMENTAL VALIDATION

A. Experimental setup

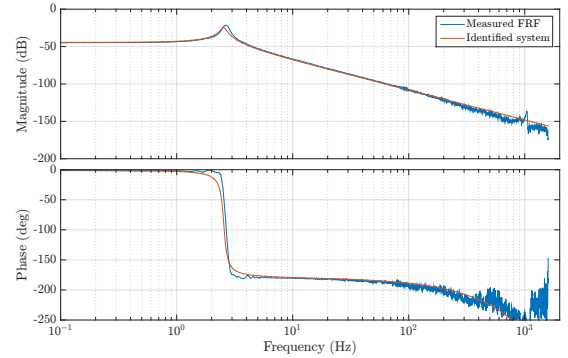
The practical system used for validation of the CRONE reset control design is a custom-designed precision stage that is actuated with the use of a Lorentz actuator. This stage is linear-guided using flexures to attach the Lorentz actuator to the base of the stage and actuated at the center of the flexures. With a *Renishaw RLE10* laser encoder the position of the fine stage is read out with 10nm resolution. A picture of the setup can be found in Fig. 7a. The controller is designed within a MATLAB/Simulink environment and implemented digitally via dSPACE DS1103 real-time control software. A sampling rate of 20kHz is used for all implemented controllers.

The frequency response of the system is shown in Fig. 7b and shows the behaviour of a second order mass-spring-damper system with additional harmonics at higher frequencies and phase lag due to delay. The transfer function of this system is identified as:

$$P(s) = \frac{0.5474}{0.5718s^2 + 0.95s + 146.3} e^{-2.5 \times 10^{-4}s}. \quad (22)$$



(a)



(b)

Fig. 7. (a) Picture of the Lorentz stage (right) with the laser encoder at the left. (b) Frequency response of the system and the identified system model.

B. Stability analysis

In this subsection the stability theory presented in previous section is applied to the designed CRONE reset controllers. As a practical example the stability analysis is shown for a CRONE-1 lag reset controller with fourth-order approximation of the fractional order (using Oustaloup approximation as in [4]), controller structure as described in section III-A and parameters as summarized in Table I.

$$\Phi_{r,\text{lag}}(\omega, p, \gamma, \omega_b, \omega_h) = \arctan \left(\frac{(1-p)\Theta_D(\gamma, \omega, \omega_b)(1 - \frac{\omega_b}{\omega_h})}{1 + (\frac{\omega}{\omega_h})^2 + \frac{\omega}{\omega_h}\Theta_D(\gamma, \omega, \omega_b)(1 - \frac{\omega_b}{\omega_h})} \right) \quad (14)$$

The open-loop responses with these reset strategies can be found in Fig. 5. In all of the strategies the open-loop shape is better with increasing non-linearity (smaller p value). For full reset ($p = 0$ and $\gamma = 0$) the gain advantage with respect to the linear CRONE controller at 1kHz is 10.9dB, 8.2dB and 7.4dB, for integrator reset, first order filter reset and lag reset respectively with bandwidth at 100Hz.

IV. STABILITY

The closed-loop system depicted in Fig. 2 is a reset system for which the following stability result holds:

Theorem 1: [16]. Let $V : \mathbb{R}^n \rightarrow \mathbb{R}^n$ be a continuously differentiable, positive-definite, radially unbounded function such that

$$\dot{V}(x) := \left(\frac{\partial V}{\partial x} \right)^T A_{cl} x < 0, \quad \text{if } e(t) \neq 0, \quad (15)$$

$$\Delta V(x) := V(A_\rho x) - V(x) \leq 0, \quad \text{if } e(t) = 0 \quad (16)$$

where A_{cl} is the closed-loop A -matrix:

$$A_{cl} = \begin{bmatrix} \bar{A} & \bar{B}C_{nrrp} \\ -B_{nrrp}\bar{C} & A_{nrrp} \end{bmatrix} \quad (17)$$

where $(\bar{A}, \bar{B}, \bar{C}, \bar{D})$ are the state-space matrices of Σ_r^* and $(A_{nrrp}, B_{nrrp}, C_{nrrp}, D_{nrrp})$ are the state-space matrices of non-reset controller Σ_{nr} and plant Σ_p combined in series, and A_ρ is defined as:

$$A_\rho = \text{diag}(\bar{A}_\rho, I_{nrrp}) \quad (18)$$

where \bar{A}_ρ is the reset matrix of Σ_r^* and n_{nrrp} is sum of the number of states of non-reset controller n_{nr} and plant n_p .

Then the reset control system is asymptotically stable.

Quadratic stability is guaranteed when (15) and (16) hold true for a potential function $V(x) = x^T P x$ with $P > 0$. From this condition the authors of [16] obtained following theorem for proving quadratic stability:

Theorem 2: [16]. There exists a constant $\beta \in \mathbb{R}^{n_r \times 1}$ and $P_\rho \in \mathbb{R}^{n_r \times n_r}, P_\rho > 0$ where n_r is the number of reset states, such that the restricted Lyapunov equation

$$P > 0, \quad A_{cl}^T P + P A_{cl} < 0, \quad (19)$$

$$B_0^T P = C_0 \quad (20)$$

has a solution for P , where C_0 and B_0 are defined by:

$$C_0 = [\beta C_{nrrp} \quad O_{n_r \times n_{nrr}} \quad P_\rho], \quad B_0 = \begin{bmatrix} O_{n_{nrrp} \times n_r} \\ O_{n_{nrr} \times n_r} \\ I_{n_r} \end{bmatrix} \quad (21)$$

and n_{nrr} is the number of non-reset states in Σ_r^* .

TABLE I
PARAMETER VALUES FOR CRONE-1 LAG CONTROLLER

Symbol	Parameter	Value
PM	phase margin	55°
ω_{cg}	bandwidth	100Hz
ω_b	lead corner frequency	12.5Hz
ω_h	lag corner frequency	800 Hz
ω_I	integrator corner frequency	8.33Hz
ω_F	low-pass filter corner frequency	1200Hz
n_I	integrator order	1
n_F	low-pass filter order	1
p	reset percentage	0.5
γ	partial reset	0.5

The non-reset control and reset control parts of the CRONE reset controller are then given by (24) and (23) respectively.

$$C_r(s) = \frac{78.54s + 3.948 \times 10^5}{5027s + 3.948 \times 10^5} \quad (23)$$

The LMI consisting of (19) to (21) for this controller and identified plant is solved using a Sedumi solver from the YALMIP toolbox in MATLAB [23], and gives a solution for $\beta = -8.99 \times 10^{-12}$ and $P_p = 0.98$. For the found P -matrix (after normalizing A_{cl}), the eigenvalues are 2.64×10^{-11} , 1.86×10^{-3} , 0.98, 1.00, 1.00, 1.00, 1.00, 1.00 and 2.00. Because the eigenvalues are all larger than zero, the found P is indeed positive definite. Thus quadratic stability is guaranteed.

VI. RESULTS

The CRONE reset controller is designed using describing function. Since reset control is non-linear, it is important to verify that the expected frequency behaviour matches actual response. For this purpose, practical frequency domain results have been retrieved. Firstly, sensitivity- and complementary sensitivity function results are discussed which are used to compute an open-loop response. Then reference-tracking results are shown for tracking an input-shaped triangular wave. Finally, time domain noise attenuation results are analysed. Since most existing work in literature is done on integrator reset and for reasons of brevity the results below are given for CRONE-1 lag reset.

A. Identification sensitivity $S(j\omega)$ and complementary sensitivity $T(j\omega)$

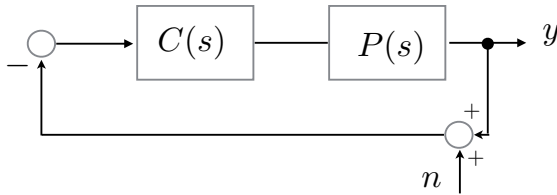


Fig. 8. Block diagram of the control loop and signals used for identification of $T(j\omega)$ and $S(j\omega)$.

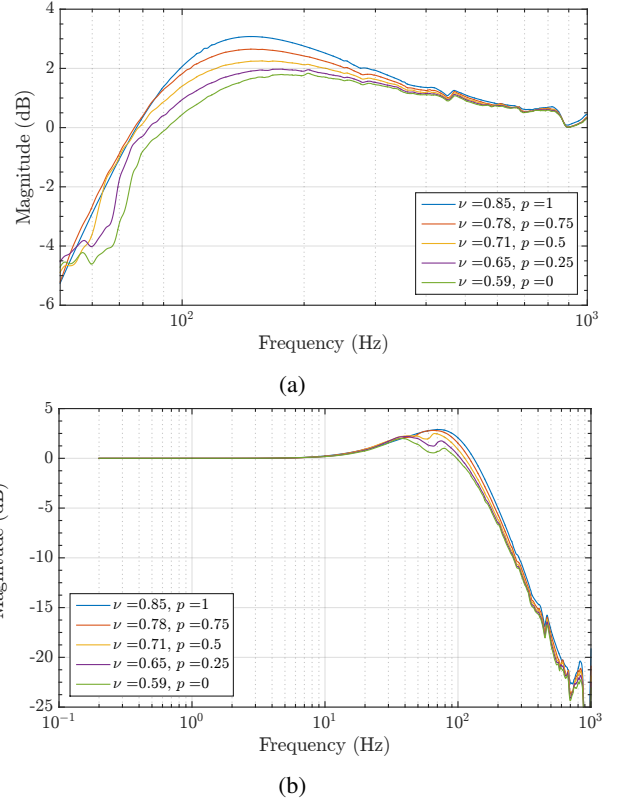


Fig. 9. (a) Sensitivity and (b) complementary sensitivity function for CRONE-1 lag reset with constant $\gamma = 0.5$ and different p -values.

Both $T(j\omega)$ and $S(j\omega)$ were identified using a frequency sweep at the position of signal n in Fig. 8. $T(j\omega)$ then can be identified as the transfer from $-n$ to y , whereas $S(j\omega)$ is identified as the transfer from n to $y + n$. The frequency sweep was done for frequencies 0.1Hz to 2.5kHz with a target time of 120s and a total duration of 480s.

$S(j\omega)$ can be found in Fig. 9a. $T(j\omega)$ is shown in Fig. 9b. As expected, noise transfer at high frequencies is reduced for lower ν and this is seen in both figures. However, for linear controllers, this would have resulted in an increase in sensitivity peak due to waterbed effect. But it is seen in Fig. 9a that with reset control, this effect is countered with the sensitivity peak below that of linear case ($p = 1$). This is also evident with complementary sensitivity in Fig. 9b where we additionally see larger decrease in gain at higher frequencies compared to linear control, hence overcoming waterbed effect.

B. Open-loop response

The open-loop responses for different CRONE-1 reset controllers were estimated by a point-wise division of identified complementary sensitivity function $T(j\omega)$ and sensitivity function $S(j\omega)$ for the same range of frequencies. This response is analysed to validate that phase margin is satisfied in all CRONE reset controllers. The identified open-loop at low frequencies up till 10Hz is considered unreliable as the coherence between the signals used for identification of the sensitivity function is poor.

$$C_{nr}(s) = \frac{2.387 \times 10^{10} s^5 + 4.589 \times 10^{13} s^4 + 2.351 \times 10^{16} s^3 + 4.084 \times 10^{18} s^2 + 2.618 \times 10^{20} s + 5.553 \times 10^{21}}{0.0285 s^6 + 530.6 s^5 + 3.267 \times 10^6 s^4 + 7.426 \times 10^9 s^3 + 5.722 \times 10^{12} s^2 + 1.175 \times 10^{15} s} \quad (24)$$

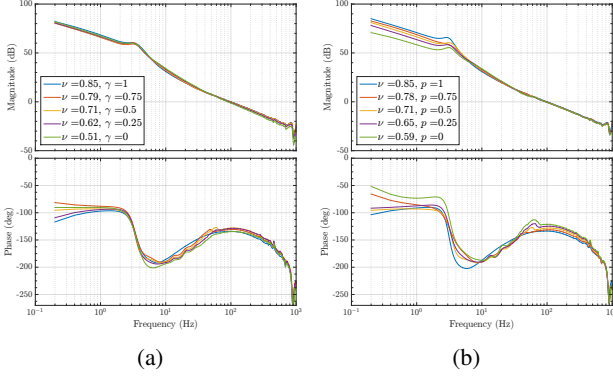


Fig. 10. Experimental open-loop responses for the system with CRONE-1 (a) lag reset with $p = 0.5$ and varying γ , (b) lag reset with $\gamma = 0.5$ and varying p .

From the experimental open-loop responses (see Fig. 10), it appears that the phase margin is larger than predicted for CRONE-1 lag reset with $\gamma = 0.5$ and varying p , as calculated ν is expected to give same phase margin. For CRONE-1 lag reset with $p = 0.5$ and varying γ the phase is approximately as predicted. Thus some relief from the Bode's gain-phase relation has been achieved.

In Fig. 9 it was observed that better noise attenuation has been achieved. Contrarily, the open-loop response shows marginal improvement in noise attenuation at frequencies above bandwidth. Also more phase lead is observed around bandwidth. We hypothesize that division between complementary sensitivity and sensitivity function does not relate directly to the open-loop response due to the non-linearity of control. However, this requires further investigation.

C. Reference-tracking

TABLE II

RMS ERROR FOR FOURTH ORDER TRIANGULAR SCANNING REFERENCE CRONE-1 LAG RESET WITH CONSTANT $\gamma = 0.5$

p	RMS error (nm)
1	480.1
0.75	424.5
0.5	385.6
0.25	353.4
0	331.5

Fourth order trajectory planning as formulated in [24] is used to create a triangular wave reference signal. This type of reference signal is representative for scanning motions in precision wafer stages. Also second order feedforward mentioned in the same paper is implemented. The maximum allowed velocity, acceleration and jerk of this reference signal are limited. As can be seen in Fig. 11, the tracking error decreases with increasing fractional order ν as predicted. The

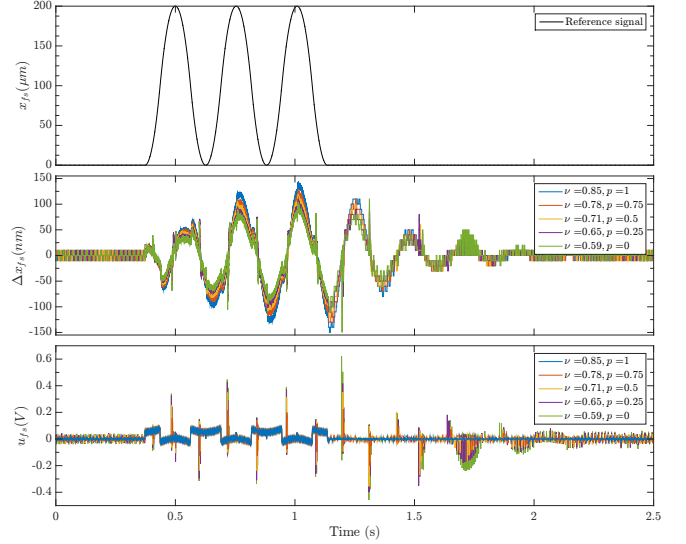


Fig. 11. Tracking of a triangular wave signal showing the reference signal, tracking error and control input for CRONE-1 lag reset with $\gamma = 0.5$ and different values for p .

RMS error values are listed in Table II and similarly show better tracking properties when more non-linearity is present in the system. Note that the maximum control input peaks increase when the system includes reset.

D. Noise attenuation

Time domain response to a sine noise signal of amplitude $2\mu\text{m}$ and frequency of 1kHz is recorded for 5s and shown in Fig. 12. It can be seen that measured output reduces for lower values of p and ν . For a range of frequencies between 300Hz and 1kHz similar reduction was observed. The decrease in average power in decibels for $p = 0$ and $\gamma = 0.5$ with respect to linear case ($p = 1$ and $\gamma = 0.5$) is shown in Table III.

TABLE III

REDUCTION OF AVERAGE POWER OF NOISE RESPONSE FOR $\gamma = 0.5$, $p = 0$ WITH RESPECT TO LINEAR CASE

Frequency (Hz)	noise reduction (dB)
300	2.85
400	2.50
500	1.90
600	2.03
700	0.86
800	2.20
900	1.84
1000	3.44

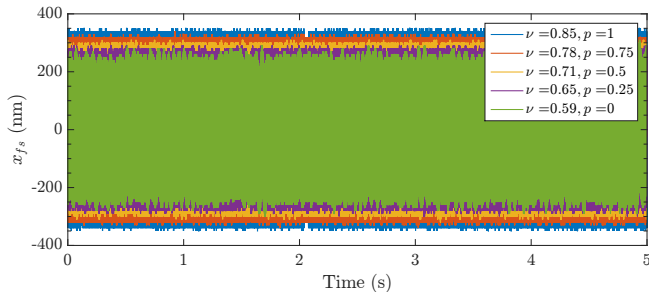


Fig. 12. Measured response for sine noise signal with frequency of 1kHz and amplitude of $2\mu\text{m}$.

VII. CONCLUSION

In the first part of this paper, a new design for fractional CRONE control with non-linear reset control was proposed. In the CRONE reset design two degrees of freedom in tuning non-linearity of the system are used to limit the control input peaks and contribution of higher harmonics.

In the second part of the paper it has been shown that when the additional phase caused by reset can be quantified, and as a result the fractional order ν of the lag filter can be decreased to the correct value, better system performance is achieved with reset compared to the linear controller for same phase margins. In the open-loop responses that were computed from practical measurements, the responses for CRONE-1 lag reset showed similar phase margins for $\gamma = 0.5$ and different p -values as well as $p = 0.5$ and different γ -values. As such they show relief from the fundamental Bode's gain-phase relation. However, further investigation of open-loop gain-behaviour in presence of non-linearities is required to explain the absence of significant increase in noise rejection and extra reset phase lead around bandwidth in the obtained open-loop response.

Several CRONE-1 lag reset controllers, satisfying quadratic stability conditions, have been implemented on a Lorentz-actuated precision stage. On this setup it was shown that tracking error decreased for more non-linearity, implying better reference-tracking of the CRONE reset controller compared to the linear CRONE controller. The identified noise transfer has reduced for frequencies measured in the range from 50Hz to 1kHz. This is supported by time domain noise measurements in which transfer of sine signals has been analysed for isolated frequencies. For all chosen frequencies between 300Hz and 1kHz noise reduction has been achieved when using CRONE reset instead of CRONE. The retrieved results show that with CRONE reset control relief from fundamental limits in linear control is possible. Having introduced loop shaping methods in the controller design, CRONE reset control is an interesting control method for making reset control more accessible to the industry.

REFERENCES

- [1] S. Skogestad and I. Postlethwaite, *Multivariable feedback control: Analysis and design*. Wiley New York, 2007, vol. 2.
- [2] K. K. Tan, T. H. Lee, and S. Huang, *Precision motion control: Design and implementation*. Springer Science & Business Media, 2007.

- [3] R. M. Schmidt, G. Schitter, and A. Rankers, *The design of high performance mechatronics - 2nd revised edition: High-tech functionality by multidisciplinary system integration*. IOS Press, 2014.
- [4] J. Sabatier, P. Lanusse, P. Melchior, and A. Oustaloup, *Fractional order differentiation and robust control design: Crone, h-infinity and motion control*. Springer, 2015, vol. 10.
- [5] M. Vidyasagar, *Nonlinear systems analysis: Second edition*, ser. Classics in Applied Mathematics. Society for Industrial and Applied Mathematics, 2002.
- [6] C. Prieur, S. Tarbouriech, and L. Zaccarian, "Improving the performance of linear systems by adding a hybrid loop," *IFAC Proceedings Volumes*, vol. 44, no. 1, pp. 6301–6306, 2011, 18th IFAC World Congress.
- [7] G. Witvoet, W. H.T. M. Aangenent, W. P.M. H. Heemels, M. J. G. van de Molengraft, and M. Steinbuch, " H_2 performance analysis of reset control systems," in *Decision and Control, 2007 46th IEEE Conference on*, IEEE, 2007, pp. 3278–3284.
- [8] Y. Li, G. Guo, and Y. Wang, "Reset control for midfrequency narrowband disturbance rejection with an application in hard disk drives," *IEEE Transactions on Control Systems Technology*, vol. 19, no. 6, pp. 1339–1348, 2011.
- [9] H. Li, C. Du, and Y. Wang, "Discrete-time H_2 optimal reset control with application to HDD track-following," in *2009 Chinese Control and Decision Conference*, 2009, pp. 3613–3617.
- [10] S. H. HosseinNia, I. Tejado, and B. M. Vinagre, "Fractional-order reset control: Application to a servomotor," *Mechatronics*, vol. 23, pp. 781–788, 2013.
- [11] L. Hazeleger, M. Heertjes, and H. Nijmeijer, "Second-order reset elements for stage control design," in *2016 American Control Conference (ACC)*, 2016, pp. 2643–2648.
- [12] J. Zheng, "Development of an extended reset controller and its experimental demonstration," *IET Control Theory & Applications*, vol. 2, pp. 866–874(8), 10 2008.
- [13] M. A. Davó and A. Baños, "Reset control of a liquid level process," in *2013 IEEE 18th Conference on Emerging Technologies Factory Automation (ETFA)*, 2013, pp. 1–4.
- [14] F. Perez, A. Baños, and J. Cervera, "Periodic reset control of an in-line pH process," in *ETFA 2011*, 2011, pp. 1–4.
- [15] J. Moreno, J. Guzmán, J. Normey-Rico, A. Baños, and M. Berenguel, "A combined FSP and reset control approach to improve the set-point tracking task of dead-time processes," *Control Engineering Practice*, vol. 21, no. 4, pp. 351–359, 2013.
- [16] A. Baños and A. Barreiro, *Reset control systems*. Springer Science & Business Media, 2011.
- [17] A. Baños, J. Carrasco, and A. Barreiro, "Reset times-dependent stability of reset control systems," *IEEE Transactions on Automatic Control*, vol. 56, no. 1, pp. 217–223, 2011.
- [18] S. J.L. M. Van Loon, K. G. J. Gruntjens, M. F. Heertjes, N. Van de Wouw, and W. P.M. H. Heemels, "Frequency-domain tools for stability analysis of reset control systems," *Automatica*, vol. 82, pp. 101–108, 2017.
- [19] S. H. HosseinNia, I. Tejado, D. Torres, B. M. Vinagre, and V. Feliu, "A general form for reset control including fractional order dynamics," *IFAC Proceedings Volumes*, vol. 47, no. 3, pp. 2028–2033, 2014.
- [20] N. Saikumar and S. H. HosseinNia, "Generalized fractional order reset element (GFrORE)," in *9th European Nonlinear Dynamics Conference (ENOC)*, 2017.
- [21] Q. Chen, Y. Chait, and C. V. Hollot, "Analysis of reset control systems consisting of a FORE and second-order loop," *Journal of Dynamic Systems, Measurement, and Control*, vol. 123, no. 2, pp. 279–283, 2001.
- [22] Y. Guo, Y. Wang, and L. Xie, "Frequency-domain properties of reset systems with application in hard-disk-drive systems," *IEEE Transactions on Control Systems Technology*, vol. 17, no. 6, pp. 1446–1453, 2009.
- [23] J. Löfberg, "YALMIP : A toolbox for modeling and optimization in MATLAB," in *In Proceedings of the CACSD Conference*, Taipei, Taiwan, 2004.
- [24] P. Lambrechts, M. Boerlage, and M. Steinbuch, "Trajectory planning and feedforward design for electromechanical motion systems," *Control Engineering Practice*, vol. 13, no. 2, pp. 145–157, 2005.